6

Integration of fibre optic sensors and sensing networks into textile structures

MAHMOUD EL-SHERIF
Drexel University, USA

6.1 Introduction

During the twentieth century, tremendous progress was made in the information and telecommunication industries. This progress can be attributed to the development of novel electronics and photonics materials. The development of semi-conductor materials and liquid crystals, processed into microstructural devices, was behind the major achievements in the information and telecommunication industries. A cell phone the size of a matchbox, that receives audio, video and e-mail messages, is an example of such progress.

In the twentyfirst century, the development of electronic and photonic textiles will form the basis for more innovations in electronics and photonics applications, ranging from communication systems and personal computers to biomedical engineering and health-monitoring equipment. Flexible cell phones or televisions with large, flexible screens, which can be folded small enough to fit into a pocket, will be developed in the near future. Health-monitoring shirts for special care will provide direct communication with the patient's physician and will feature feedback control of a through-the-skin drug delivery system. A clip-on textile patch will be used as a cell phone; without using one's hands, one will be able to communicate with anyone, anywhere. Car seats will talk to the passenger to provide comfortable conditions. Uniforms for fire fighters, security guards and special mission personnel will provide all of the information required for their safety and security, as well as transmit remotely information on their health and environmental conditions to a central command facility (El-Sherif, 1997). Novel electronic and photonic systems will be developed that can take advantage of flexible electronic textiles that can conform to the shape of any structure on the ground, in space or under water.

'Smart' textiles are an interesting class of electronics and photonics textiles. They are defined as textiles capable of monitoring their own 'health' conditions and structural behaviour, as well as sensing external environmental conditions and

sending the information to other locations. They consist of special types of sensors, signal processors and communication networks embedded into a textile substrate. The conventional sensors and networking systems that are currently available are not technologically mature enough for such applications. New classes of miniature sensors, signal processing devices, and networking links are therefore urgently needed for such applications, and methods for integrating these devices into textile structures need to be developed (El-Sherif *et al.*, 1999).

Responding to the challenges inherent in the development of smart textiles, a highly qualified team was organised in the mid-1990s by the Fibre Optics and Photonics Center of Drexel University and Photonics Laboratories Inc., Philadelphia, Pennsylvania. The team focused on developing a new class of smart textiles composed of integrated fibre optic sensors and networks. Optical fibres are compatible with textile structures and thus present the best choice for the time being. The development of smart textiles requires extensive multidisciplinary research and development (R&D) in textiles and materials engineering, as well as fibre optics and electrical engineering.

A novel case study, based on three major research projects, will be presented in this chapter. These projects focused on the following:

- smart textiles with embedded optical fibres and electric wires for networking and information transmission
- a smart parachute with embedded fibre optic sensors for measuring dynamic structural behaviour during inflation and airdrops
- smart uniforms with embedded fibre optic sensors for detecting environmental conditions and biological threats.

Through these projects, new theories and technologies related to the development of smart textile structures were developed. The R&D work that was conducted ranges from structural design, modelling and analysis to the processing, manufacturing and testing of samples of smart textiles. Specifically, special types of compatible and miniature fibre optic sensors were developed. The methodology to integrate these sensors, as well as optical fibres and fine electrical wires, into various textile-based structures (knitted, woven and non-woven) is under investigation. Integrating lightweight flexible sensors and networks into smart textiles will provide tremendous advantages for many applications. This integration will form the basis for the future development of flexible optoelectronic devices and systems. A number of PhD dissertations and MS theses have been completed, and many technical reports and papers have been published, recording the progress achieved so far.

This chapter is organised into four main sections. The first section presents a short introduction to the design of smart textile structures. To identify the structural design parameters, a new model has been developed for structural analysis and will be discussed in the second section. The third section presents the methodologies that have been developed for integrating optical fibres and electric wires into

various textile structures. The last section focuses on the application of smart textiles. The applications are based on the integration of fibre optic sensors and networks into the textile structure to monitor the structural behaviour and environmental conditions. Specifically, two applications are under study. The first involves using a smart parachute canopy to measure the dynamic structural behaviour of parachutes during airdrops and inflation. The second concerns the development of smart uniforms capable of monitoring environmental conditions. These applications require the development of special types of compatible sensors. In the last section, a brief introduction of such sensors, which are strain/stress and chemical sensors, is also presented.

6.2 Smart textiles

The development of smart textiles with embedded optical fibres and electric wires requires a full understanding of the structural behaviour and geometry of textiles. For the proper integration of optical fibres, the processing parameters and final shape conditions of the textile structures need to be carefully identified. Three types of basic textile structures (knitted, woven and non-woven) are under consideration for development as smart textiles.

6.2.1 Knitted structures

There are two main types of knitted structures, warp knitted and weft knitted, as shown in Fig. 6.1. The yarns in a knitted textile material are in the form of interloops that are subjected to very tight bends at a very small radius of curvature. The idea of replacing one of the yarns with optical fibre is not acceptable for these structures. The tight bends may cause extreme losses in optical signals and may even result in their mechanical failure. Therefore, optical fibres used in knitted

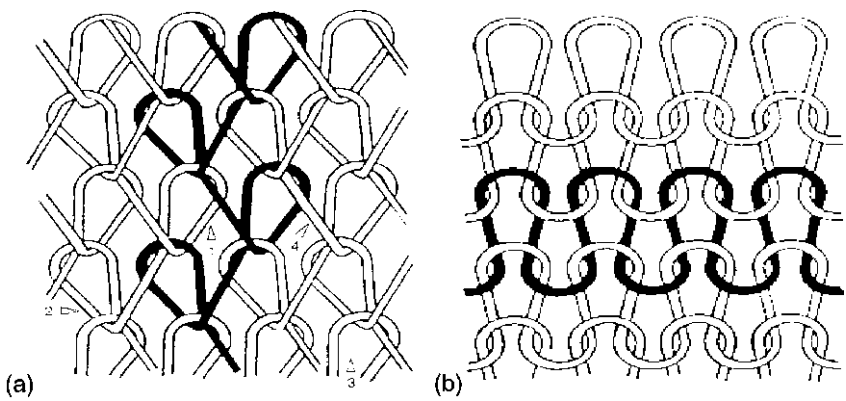

6.1 Knitted textile structure, warp knitted (a) and weft knitted (b).

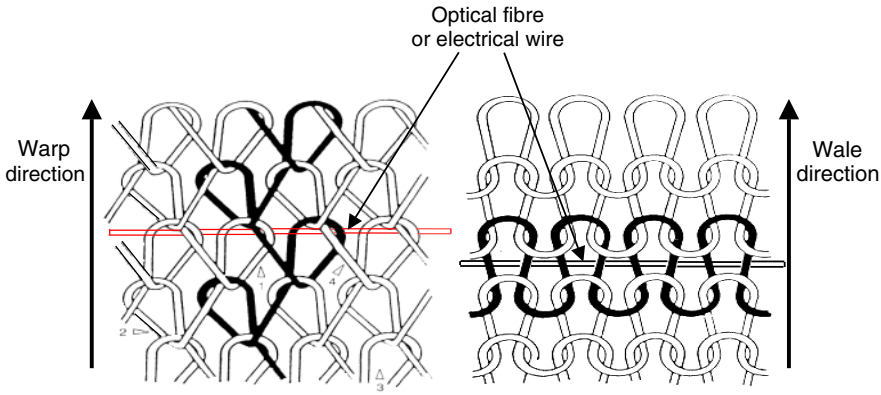

6.2 Optical fibre or electronic wire integrated into the warp (left) or weft (right) textile knitted structures.

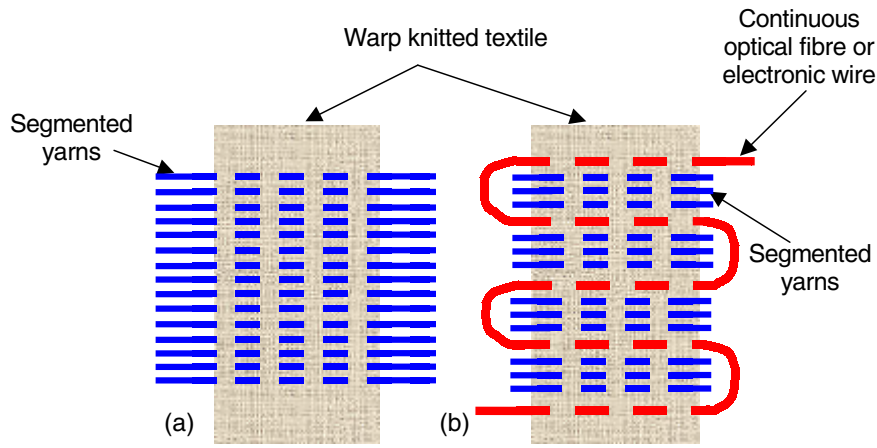

6.3 Schematic diagrams of (a) segmented yarns and (b) continuous optical fibre or wire, taking a serpentine shape.

structures cannot be intertwined in the same way as textile yarns. However, optical fibres and electric wires can be integrated in a straight line, interlacing with the loops. It is possible to integrate optical fibres and wires in a weft or warp knitted textile, as shown in Fig. 6.2. In this case, the integrated optical fibres and wires can have an acceptable path in the textile material without critical bending and mechanical deformation.

To construct a network of optical signals within textile structures, optical fibres and wires must be integrated in a continuous way and not in short segments, as is the case with the yarns shown in Fig. 6.3(a). One of the integration patterns of fibres/wires is in a serpentine shape, as shown in Fig. 6.3(b). Optical fibre can replace some of the segmented yarns at certain locations. The integrated patterns

have to be designed to have a bending curvature of fibres/wires larger than their critical values and also to be suitable for use in knitting machines.

6.2.2 Woven structures

In woven textiles, there are three forms of woven structures: plain, twill and satin. The yarns are interlaced and subjected to bending, as shown in Fig. 6.4. In these woven structures, the yarns are subjected to high bending density. The twill weave, however, has less of a bending curvature than plain or satin structures. Twill yarns, with patterns such as 2/2 or 4/4, could interlace after crossing every two or more strands of transverse yarn. Also, the satin weave has a less dense interlacing structure than the plain weave. The satin weave yarns interlace over or under only one strand of transverse yarn, and then cross two or more strands of transverse yarn. For example, the four-harness weave would interlace over one strand of transverse yarn and then cross four strands of transverse yarn. Therefore, in woven structures, the best integration of optical fibres is in twill weave structures, where the fibre is subjected to the least amount of bending in the curvature. Figure 6.5 presents a cross-sectional view of different weaving structures. Optical fibres (or electric wires) can be integrated in any woven structure in the warp and weft directions, as shown in Fig. 6.6. For example, one of the strands of transverse yarn can be replaced by an optical fibre or electric wire, as shown in Fig. 6.5. However, the best condition for integration is the one with the least bending angles.

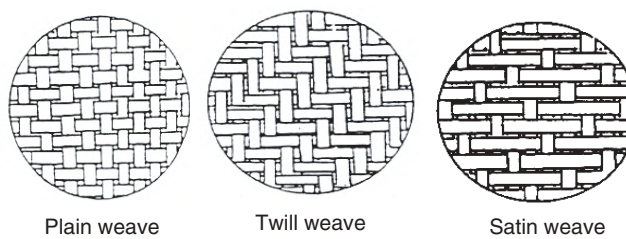

6.4 Three forms of weaving structures.

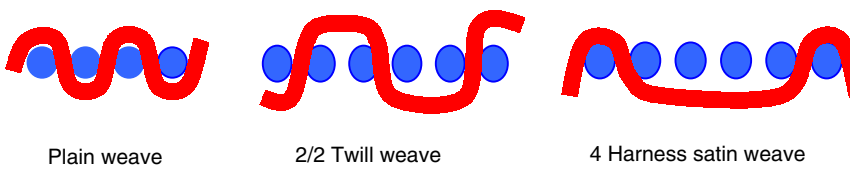

6.5 Cross-sectional view of different weaving structures.

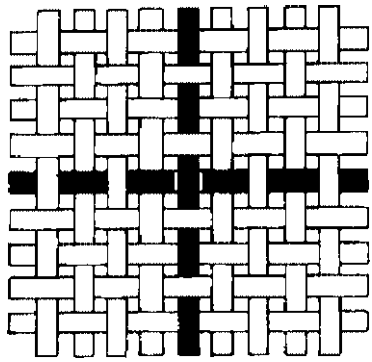

6.6 Optical fibre or wire integrated into a woven fabric in the warp and weft direction.

6.2.3 Non-woven structures

Non-woven textiles are made up of sheet materials composed of more or less randomly oriented segments of fibre bonded together. There are basically two structural features in non-woven structures: the mode of web formation and the mode of bonding. The most common web formation consists of layers of short fibres laid on top of each other. For non-woven structures there are three main types of bonding: entanglement, sticking the fibres together and stitching through the fabric. Thus, the only way for optical fibres and electric wires to be integrated is to place them between sheets (or layers). The orientation of fibres/wires can be in a straight line or with minimum bending curvature. Therefore, the integration of optical fibres in non-woven structures is much easier than in knitted or woven structures.

6.2.4 Studying the machinery

To integrate optical fibres and wires in various textile structures, one must also understand the machinery used in the process. It is very important to evaluate the mechanical motion configuration and process stress parameters exerted on textile yarns during the manufacturing process to achieve the successful integration of optical fibres and wires. Understanding the mechanics involved in the process is essential to selecting the proper way to integrate optical fibres or to modify the process to meet the requirements of optical fibres. Modifications of the process can be achieved by adding an additional track, as a feeder for optical fibres or electric wires. Different types of machines used to manufacture knitted, woven and non-woven fabrics were studied. It was found that some of the mechanical parts, which produce sharp bending in textile fibres during the process, as shown in Fig. 6.7,

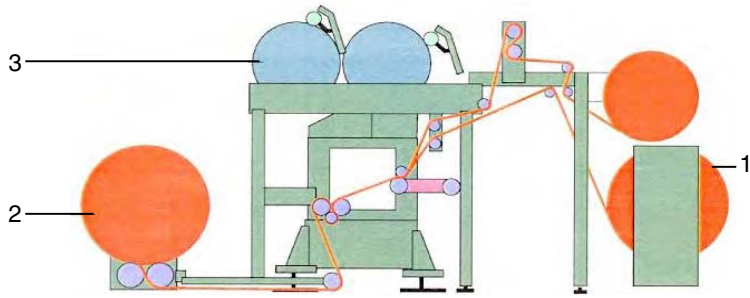

6.7 Schematic diagram of a textile machine, showing the motion of the fabrics/yarns through the major parts (1-2-3), during the manufacturing process.

may need to be modified to limit the angle of the bending of the fibres, as required for optical fibres. Therefore, a study of the machinery may need to be carried out to provide the base of knowledge from which to modify properly the components to adapt the manufacturing process to the requirements of optical fibres.

6.3 Modelling and analysis

Bending is one of the major problems in the integration of optical fibres/wires into textile fabrics, not only during the process but also for the final shape and use of the finished product. Bending may induce mechanical damage and signal loss in optical fibres. Although the bending of optical fibres/wires is a complicated problem, investigations both in theoretical and experimental aspects are very important for the proper design and manufacturing of smart textiles. Therefore, if smart textiles are to be properly designed, the fibre-bending conditions need to be predicted. Unfortunately, the available theories on the design of textile structures are not sufficiently developed to allow predictions of the actual bending angles and curvatures of the yarns at various locations in the textile structures. Optical fibres can be bent within a certain limit without leading to the loss of signals or damage to the fibres. To predict accurately the bending conditions of optical fibres integrated into textile structures, a textile fabric model has been developed. The developed model is designed for a general plainly woven shape; however, it can be modified for application to other textile structures. A plain-weaving unit cell is shown in Fig. 6.8. The diameter of the filling yarns is different from that of the warp yarns. Optical fibre can replace any of these yarns.

This model can be used to predict the geometrical shape and bending of the optical fibres to analyse the effect of the textile's structure on signal processing. In developing this model, relationships of both geometrical and mechanical equilibrium between yarns are considered (Hearle *et al*., 1969; Olofsson, 1964;

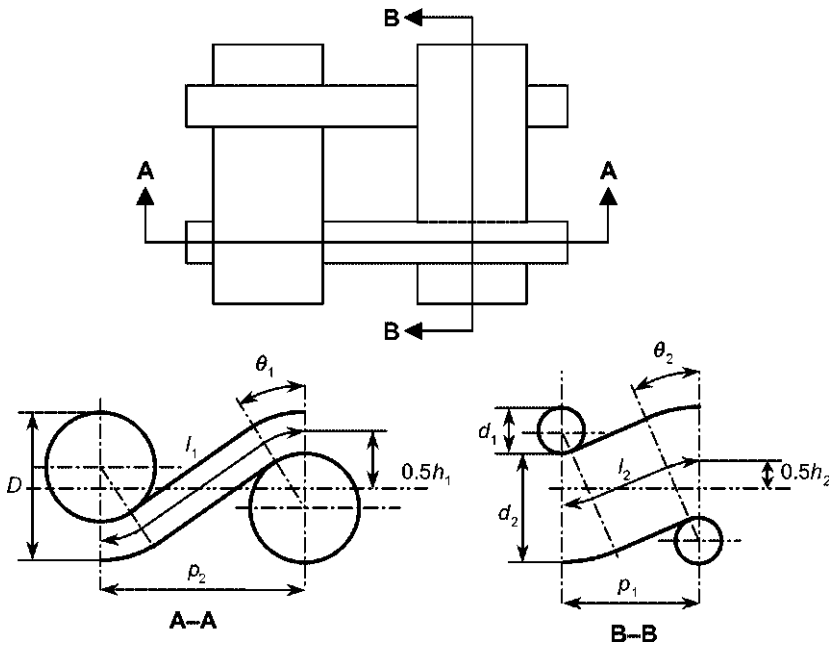

6.8 Orthogonal unit cell showing interlacing geometry for plain weaving structure.

Peirce, 1937). Six equations have been used to govern the orthogonal interlace both geometrically and mechanically. In the calculation to solve the unknown, the Newton–Raphson iteration algorithm (Olofsson, 1964) has been adopted to treat non-linear algebraic equations, and the computer program to perform the calculation has been implemented using C++ computer language. The numerically calculated results have been compared with those from other models.

In this model, circular cross-sectional yarns/fibres, uniform structure and isotropic material properties are assumed. An orthogonal interlace cell consisting of straight and circular portions has been selected to undergo both geometrical and mechanical analyses under the model. The model and the corresponding parameters of the unit cell are shown in Fig. 6.8.

The Peirce geometrical model (Peirce, 1937) gives the following:

$$p_1 = (l_2 - D\theta_2)\cos\theta_2 + D\sin\theta_2 \quad [6.1]$$

$$p_2 = (l_1 - D\theta_1)\cos\theta_1 + D\sin\theta_1 \quad [6.2]$$

$$h_1 = (l_1 - D\theta_1)\sin\theta_1 + D(1 - \cos\theta_1) \quad [6.3]$$

$$h_2 = (l_2 - D\theta_2)\sin\theta_2 + D(1 - \cos\theta_2) \quad [6.4]$$

$$D = h_1 + h_2 \quad [6.5]$$

Applying force equilibrium yields:

$$m_1 p_1^2 \sin\theta_1 = m_2 p_2^2 \sin\theta_2 \qquad [6.6]$$

where l_1 is the warp length between two adjacent filling threads (l_1 is not smaller than $D\theta_1$), l_2 is the filling length between two adjacent warp threads (l_2 is not smaller than $D\theta_2$), p_1 is the warp spacing, p_2 is the filling spacing, θ_1 is the weave angle of warp yarn to the plane of the cloth ($0 \le \theta_1 \le 0.5\pi$), θ_2 is the weave angle of the filling yarn to the plane of the cloth ($0 \le \theta_2 \le 0.5\pi$), h_1 is the displacement of the normal axis of the warp yarn to the plane of the cloth, h_2 is the displacement of the normal axis of the filling yarn to the plane of the cloth, m_1 is the bending rigidity of the warp yarn, m_2 is the bending rigidity of the filling yarn, $D = d_1 + d_2$ = effective thickness of the fabric, d_1 is the diameter of the warp yarn, and d_2 is the diameter of the filling yarn.

Six independent equations can be used to solve six unknowns. To demonstrate the method, the six unknowns are assumed to be l_1, l_2, h_1, h_2, θ_1 and θ_2. The rest of the parameters are all known values. The Newton–Raphson iteration algorithm has been adopted to treat the non-linear algebraic equations, Equation [6.1] through Equation [6.6]. The equations for solving the problem in matrix form have been derived as follows:

$$\begin{pmatrix} \frac{\partial F_1^i}{\partial l_1^i} & \frac{\partial F_1^i}{\partial \theta_1^i} & \frac{\partial F_1^i}{\partial h_1^i} & \frac{\partial F_1^i}{\partial h_2^i} & \frac{\partial F_1^i}{\partial l_2^i} & \frac{\partial F_1^i}{\partial \theta_2^i} \\ \frac{\partial F_2^i}{\partial l_1^i} & \frac{\partial F_2^i}{\partial \theta_1^i} & \frac{\partial F_2^i}{\partial h_1^i} & \frac{\partial F_2^i}{\partial h_2^i} & \frac{\partial F^i{}_2}{\partial l_2^i} & \frac{\partial F_2^i}{\partial \theta_2^i} \\ \frac{\partial F_3^i}{\partial l_1^i} & \frac{\partial F_3^i}{\partial \theta_1^i} & \frac{\partial F_3^i}{\partial h_1^i} & \frac{\partial F_3^i}{\partial h_2^i} & \frac{\partial F_3^i}{\partial l_2^i} & \frac{\partial F_3^i}{\partial \theta_2^i} \\ \frac{\partial F_4^i}{\partial l_1^i} & \frac{\partial F_4^i}{\partial \theta_1^i} & \frac{\partial F_4^i}{\partial h_1^i} & \frac{\partial F_4^i}{\partial h_2^i} & \frac{\partial F_4^i}{\partial l_2^i} & \frac{\partial F_4^i}{\partial \theta_2^i} \\ \frac{\partial F_5^i}{\partial l_1^i} & \frac{\partial F_5^i}{\partial \theta_1^i} & \frac{\partial F_5^i}{\partial h_1^i} & \frac{\partial F_5^i}{\partial h_2^i} & \frac{\partial F_5^i}{\partial l_2^i} & \frac{\partial F_5^i}{\partial \theta_2^i} \\ \frac{\partial F_6^i}{\partial l_1^i} & \frac{\partial F_6^i}{\partial \theta_1^i} & \frac{\partial F_6^i}{\partial h_1^i} & \frac{\partial F_6^i}{\partial h_2^i} & \frac{\partial F_6^i}{\partial l_2^i} & \frac{\partial F_6^i}{\partial \theta_2^i} \end{pmatrix} \begin{pmatrix} \Delta l_1^i \\ \Delta \theta_1^i \\ \Delta h_1^i \\ \Delta h_2^i \\ \Delta l_2^i \\ \Delta \theta_2^i \end{pmatrix} = - \begin{pmatrix} F_1^i \\ F_2^i \\ F_3^i \\ F_4^i \\ F_5^i \\ F_6^i \end{pmatrix} \qquad [6.7]$$

where the entries of the right column in Equation [6.7] are given in Equation [6.8]:

$$\begin{cases} -F_1^i = p_2 - (l_1^i - D\theta_1^i)\cos\theta_1^i - D\sin\theta_1^i \\ -F_2^i = h_1^i - (l_1^i - D\theta_1^i)\sin\theta_1^i - D(1-\cos\theta_1^i) \\ -F_3^i = D - h_1^i - h_2^i \\ -F_4^i = h_2^i - (l_2^i - D\theta_2^i)\sin\theta_2^i - D(1-\cos\theta_2^i) \\ -F_5^i = p_1 - (l_2^i - D\theta_2^i)\cos\theta_2^i - D\sin\theta_2^i \\ -F_6^i = \dfrac{m_1}{m_1}\left(\dfrac{p_1}{p_1}\right)\sin\theta_1^i - \sin\theta_2^i \end{cases} \quad [6.8]$$

The entries of the matrix in Equation [6.7] are given in Equation [6.9]. Therefore, the terms in Equation [6.8] are substituted, and the matrix given by Equation [6.7] becomes Equation [6.9]:

$$\begin{pmatrix} \cos\theta_1^i & (D\theta_1^i - l_1^i)\sin\theta_1^i & 0 & 0 & 0 & 0 \\ \sin\theta_1^i & (l_1^i - D\theta_1^i)\cos\theta_1^i & -1 & 0 & 0 & 0 \\ 0 & 0 & -1 & -1 & 0 & 0 \\ 0 & 0 & 0 & -1 & \sin\theta_2^i & (l_2^i - D\theta_2^i)\cos\theta_2^i \\ 0 & 0 & 0 & 0 & \cos\theta_2^i & (D\theta_2^i - l_2^i)\sin\theta_2^i \\ 0 & -\dfrac{m_1}{m_2}\left(\dfrac{p_1}{p_2}\right)^2\cos\theta_1^i & 0 & 0 & 0 & \cos\theta_2^i \end{pmatrix} \begin{pmatrix} \Delta l_1^i \\ \Delta\theta_1^i \\ \Delta h_1^i \\ \Delta h_2^i \\ \Delta l_2^i \\ \Delta\theta_2^i \end{pmatrix} = \begin{pmatrix} F_1^i \\ F_2^i \\ F_3^i \\ F_4^i \\ F_5^i \\ F_6^i \end{pmatrix} \quad [6.9]$$

The solution for Equation [6.9] is obtained through iteration, where the superscript i is the iteration counter, such as in $l_1^{i+1} = l_1^i + \Delta l_1^i$. The convergence of the solution during the process of iteration is measured by the fraction of the Euclidean norm, and the iteration will be terminated when it satisfies the required tolerance (*Tor*). Note that any non-zero estimate for the unknowns can be used as an initial estimate.

To demonstrate the validity of the model, the numerical calculations were performed using self-developed software (FABCAL v2.0). The result based on the current model was compared with the result from either the Peirce model (Peirce, 1937) or the Olofsson model (Olofsson, 1964). If the desired tolerance is set to *Tor* = 10^{-8}, it only takes about six or seven iterations to make the solution converge within a second in most current personal computers. After the solution is obtained, the warp crimp c_1 and filling crimp c_2 can be readily calculated using the following equations:

$$c_1 = \frac{l_1}{p_2} - 1 \quad [6.10]$$

$$c_2 = \frac{l_2}{p_1} - 1 \qquad [6.11]$$

In addition, the bending force can be calculated as:

$$S_1 = S_2 = \frac{\pi E_1 d_1^4 \sin\theta_1}{8p_2^2} = \frac{\pi E_2 d_2^4 \sin\theta_2}{8p_1^2} \qquad [6.12]$$

where E_1 = Young's modulus of the warp yarn and E_2 = Young's modulus of the filling yarn.

In summary, based on this developed model and the numerical analysis performed, the bending angle of embedded optical fibres can accurately be predicted for various woven structures (Zhao *et al.*, in press). As soon as the bending angles are known, the transmission of optical fibres can be evaluated theoretically and experimentally, before the fibres are integrated in textile structures. Also, proper fibre materials can be selected based on geometrical–mechanical system parameters.

6.4 Manufacturing of smart textiles

In developing the methodology to integrate fibres/wires, the proper fibre/wire must first be identified and selected. The optical, mechanical and electrical properties of these fibres/wires must be characterised. One of the major issues in the process of integration is the bending condition of the fibres/wires during the manufacturing process and in the final textile products. Bending with a small curvature on the fibre/wire may result in high optical loss or in increasing the wire resistance and even breaking of the fibre/wire. Thus, critical bending parameters have to be defined for different types of fibres/wires before the fibres/wires are applied in the process of integration. Therefore, techniques for evaluating optical fibres and electric wires have to be developed. In this section, newly developed testing methods are discussed and a number of examples of the integration of fibres/wires in knitted, woven and non-woven textiles are presented.

Different types of warp knitting machines (or weft knitting) have the capability to integrate optical fibres into the filling direction of the fabric during the knitting process. The optical fibres can be integrated at specific intervals of time using the machine's software program. Specific time intervals for feeding can be set for different kinds of integration processes to limit the bending curvature at the end of the lines.

With regard to weaving machines, most such advanced machines are computerised and can be used to produce plain, twill or satin woven structures with different patterns and densities of yarn. The yarn density is expressed as picks per inch (PPI). A large number of samples were manufactured. The yarn densities of the processed samples ranged from 25 to 200 PPI. Regular textile machines were used

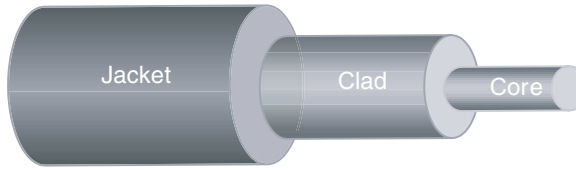

6.9 Schematic of optical fibre.

with no modification or with minor modification by adding an extra loom for the integration of optical fibres/wires.

Non-woven fabrics are produced by heat bonding or by stitching the polyester sheets together. In this case, optical fibres can be embedded between the sheets. The whole layered sample is then fed into a heated roller machine. In another process, the bonding of the polyester sheets is achieved by using a binder, while the optical fibre is positioned between the sheets.

6.4.1 Selection and testing of optical fibres and electric wires

Optical fibres

Optical fibres are cylindrical dielectric waveguides, consisting of three layers, in general, the core, cladding and coating/jacket layers, as shown in Fig. 6.9. The core and cladding are both made of dielectric transparent materials. Both ceramic materials, such as silica and alumina, and polymers, such as polystyrene and polymethyl methacrylate (PMMA), can be used as core or cladding materials. The coating/jacket is used to protect and mechanically support the fibres; thus, they are made of non-transparent polymers and may consist of more than one layer.

The optomechanical properties of the fibres are the major characteristics considered in smart textile applications. The selected fibres have to have the properties of flexibility and small bending loss. There are many types of fibres on the market, from single-mode to multimode fibres, and from all-silica to all-polymer fibres, with a variety of combinations of material properties and core and cladding geometry. The values of the fibre in terms of Young's modulus, maximum strength and Poisson's ratio are important parameters for embedded applications.

Different models have been developed to estimate the bending loss in single-mode or multimode fibres. Since bending is a complicated problem, these models are based on certain assumptions and are fairly complex. Therefore, the experimental testing of specific types of fibres is very important in determining the limitations of bending. In general, when the bending radius is less than the critical bending radius, there is a dramatic increase in bending loss. Since no previous work has appeared in the literature explaining how these tests can be conducted or

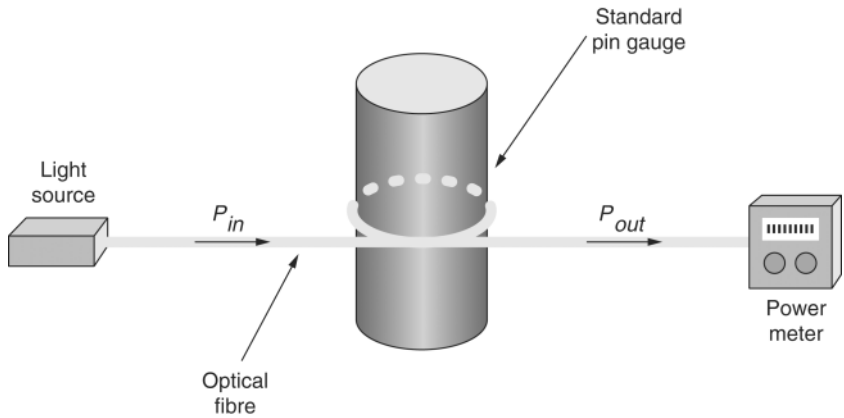

6.10 Experimental setup of bending loss measurement for optical fibres.

discussing any similar applications, part of this study is concerned with ways of developing the testing methods and standard parameters for weaving optical fibres into textile structures.

Different types of (compatible) single-mode and multimode fibres were selected and tested for their optical signal loss at different bending curvatures. An experimental setup was designed for a test of bending loss in fibres, as shown in Fig. 6.10. The optical fibre is wrapped around a standard pin gauge. A light source is connected to the fibre from one end and a power meter is connected to the other end. For each type of fibre, a test was performed at a different bending radius (R) and a different number of turns around standard pin gauges. The diameter of the standard pin gauges used ranged from 25 to 2.5 mm.

Since bending loss in fibres is related to the wavelength of transmitted light, both a 850 nm and a 1550 nm light source were used to test each type of fibre. The test was applied to a large number of fibres to study the behaviour and properties of each under various bending conditions. The optical signal loss induced by wrapping each fibre one cycle around different sizes of standard pin gauges was measured and recorded. Samples of the test results performed on five multimode optical fibres at 850 nm are shown in Fig. 6.11, and the general properties of those fibres are listed in Table 6.1 for comparison. These fibres all have different geometries and different material properties.

The optical loss for a number of cycles (n) at a specific bending diameter (d) is calculated according to the following equation:

$$\alpha(nd) = -10\log\frac{P}{P(nd)}$$

where P and $P(nd)$ are the output powers before and after the fibre is wrapped (n) turns around standard pin gauges of diameter (d), respectively.

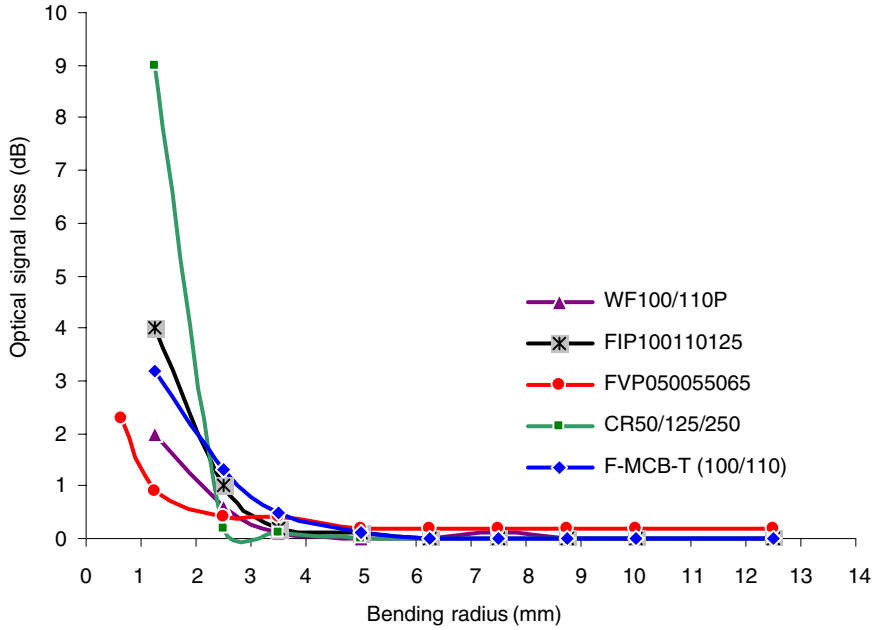

6.11 Optical signal loss of five types of multimode (MM) fibres, measured at different bending curvature using 850 nm light source.

It can be inferred from Fig. 6.11 that the loss is negligible for all selected multimode (MM) fibres when their bending curvature is larger than 5 mm; however, the loss of different types of fibres shows diversity when they are bent smaller than 5 mm. For one fibre, FVP050055065, optical loss starts to increase quickly when the bending radius is smaller than 2 mm. However, mechanical testing shows that this fibre can be bent to 0.625 mm without experiencing mechanical failure or breaking. The critical bending radii (defined as the value when fibre optical bending loss starts to increase) of the other four types of fibres,

Table 6.1 Properties of the multimode optical fibres shown in Fig. 6.11

Fibre part number	Size (core/clad/jacket) (μm)	Materials (core/clad/jacket)	NA	Tensile stress (kpsi)
FVP050055065	50/55/65	Silica/silica/polyimide	0.22 (sp)	100
FIP100110125	100/110/125	Silica/silica/polyimide	0.22 (sp)	100
CR50/125/250	50/125/250	Silica/silica/acrylate	0.20 (gd)	100
WF100/110P	100/110/135	Silica/silica/polyimide	0.22 (sp)	70
F-MCB-T	100/110/140	Silica/hard-polymer/tefzel	0.22 (sp)	100

sp = step index fibre; gd = graded index fibre.

Table 6.2 Commercial specifications of enamel-coated magnet wires

Wire type (gauge)	Measured resistivity ($10^{-8}\ \Omega \cdot m$)	Diameter of wire (mm)	Color of coating
22	1.3	0.67	Gold
26	1.9	0.42	Green
30	2.1	0.27	Red

shown in Fig. 6.11, are 3.5 mm for fibres F-MCB-T, WF 100/110P and FIP100110125; and 2.5 mm for fibre CR50/125/250. After all of the fibres have been optically and mechanically tested and the results analysed, it became clear that the materials of the fibre as well as the thickness of the cladding/coating are both important parameters in evaluating the critical bending radius of the fibre. These results were used to select the most compatible fibres for integration into textile structures (El-Sherif, 2002a).

Electric wires

Copper wires with a cylindrical shape are the most common wires used in electronic components. Therefore, samples of these wires were selected for integration with textiles; however, twisted and coaxial wires were also considered for future applications. Three types of enamel-coated wires (listed in Table 6.2) each having a different resistance, diameter and colour of coating were selected for integration into textile fabrics.

The resistances of these electronic wires have been measured at different bending curvatures (from 25 to 1.25 mm). There was no change in resistance for both the 30 gauge and the 26 gauge wires throughout the experiment on bending curvatures. However, the 22 gauge wire (the thickest) shows no change in resistance for all bending diameters larger than 5 mm. For a bending of less than 5 mm, the 22 gauge experiences a gradual increase in resistance, up to 50% at a bending radius of 1.25 mm (El-Sherif, 2002a).

6.4.2 Integration of optical fibres and electric wires into textiles

Several types of basic textile structures were used for the integration of optical fibres and electric wires. Such structures are warp knitting and weft knitting; plain, twill and satin weaving; and the non-woven fabrics produced by either heat bonding or adhesive bonding. The process of integrating optical fibres and wires into those textile structures would be fully automated in large-scale manufacturing. There are three requirements for a successful method of integration:

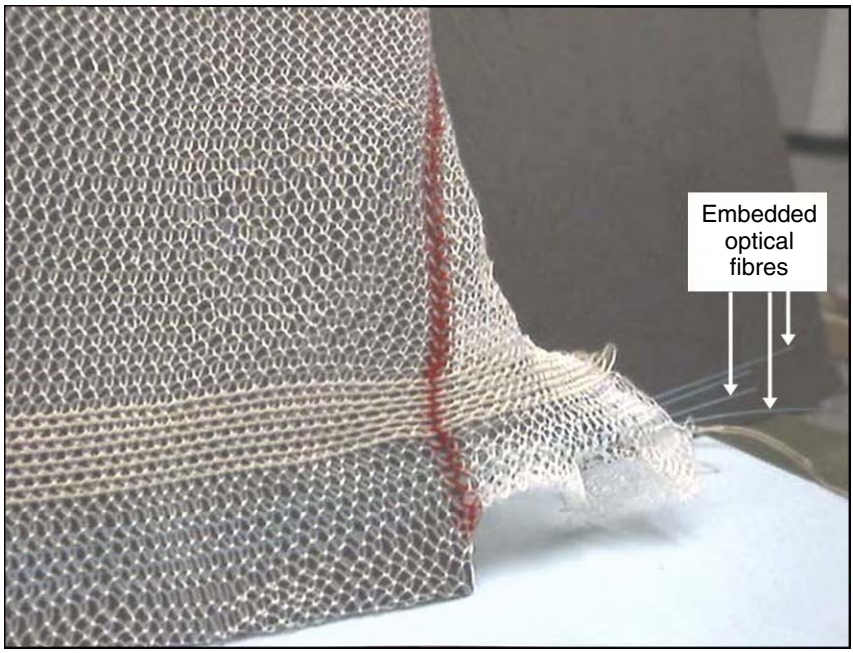

6.12 Optical image of a knitted fabric with embedded optical fibres.

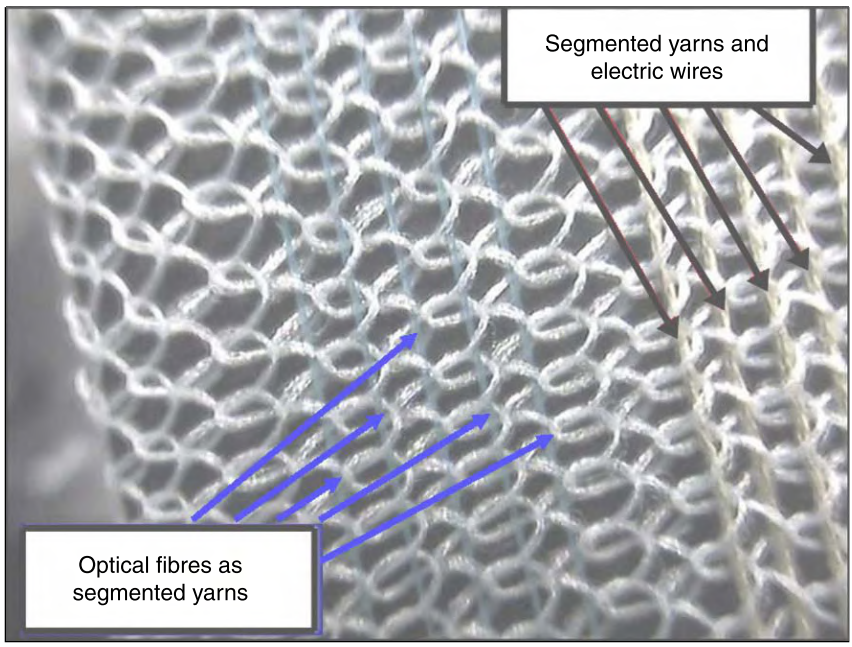

6.13 Closer look at optical fibre/wires integrated into knitted textile.

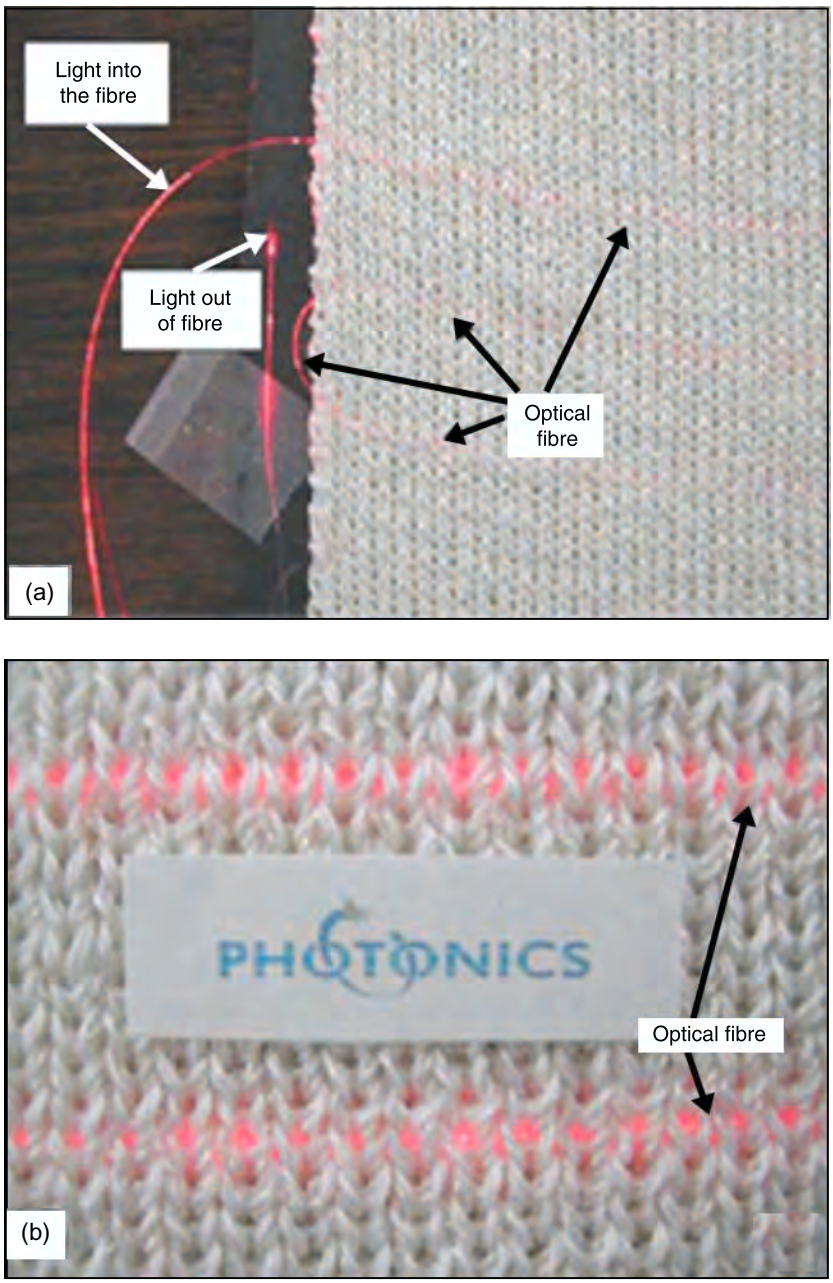

6.14 (a) Optical fibre integrated into a weft knitted textile in a serpentine shape and (b) a magnified part of (a).

1 The process of integration has to be applied to large-scale manufacturing.
2 The optical fibres and electrical wires should not show any signs of damage or signal weakness during the manufacturing process.
3 The application of the final product should not change the signal propagation more than the values indicated in the the predesigned conditions.

A study conducted recently has proven that the continuous integration of fibres/wires can be achieved through the ordinary operation of textile machines. Different types of selected optical fibres and electronic wires were successfully incorporated into knitted, woven and non-woven fabrics. Signal processing tests show that the developed methodologies have an almost negligible effect on the transmission of signals through the integrated fibres or wires.

Optical fibres and electronic wires can be integrated into knitted fabrics along the weft direction in short segments or continuously in a serpentine shape. Figures 6.12 and 6.13 show a sample of a weft knitted fabric with a number of optical fibres and electric wires integrated in the fabric as segmented yarns, and Fig. 6.14 shows a sample of the continuous feeding of the optical fibre in a serpentine shape. A specific time interval was set in order to create an acceptable serpentine shape of the bending curvature of the optical fibre (El-Sherif, 2002a). This method helped to avoid signal losses.

In order to insert an optical fibre and a wire into a woven textile, the fibre and wire must be woven into the structure just as the yarns are woven. In any weaving machine, the yarns in the warp direction are pulled out from a roller that contains many individual strands of yarns. These yarns are then formed into a woven structure by passing a strand of yarn in the transverse or weft direction via a shuttle, which interlaces the yarns. Significantly, the yarns in the weft direction are not continuous and their length cannot be very long since this length would match the width of the weaving machine. However, the yarns in the warp direction are much longer than those in the weft direction, since these yarns are continuously pulled out of a roller.

A very long piece of fibre/wire can be integrated into the fabric in the warp direction during the weaving process, as shown for the transverse yarn in Fig. 6.15 for a satin woven structure. In addition, the density of optical fibres and wires in the textile structure can be easily controlled. Therefore, in woven fabrics, optical fibres and wires are processed as warp yarns. The integrated fibre/wire took the exact same path as one of the yarns fed from the roller in the warp direction. Several samples were processed with fabric densities ranging from 25 to 200 PPI. The higher the density, the tighter was the structure of the fabric. A sample of a plain-woven fabric at 80 PPI is shown in Fig. 6.16. In this fabric, two optical fibres and two electric wires were integrated into the warp direction. Integrated fibres/wires interlace with a strand of one-weft yarn once with every strand of seven-weft yarn. The integration of fibres/wires did not influence the regular weaving procedure or the structure of the fabric because the integrated fibre/wire was treated as the

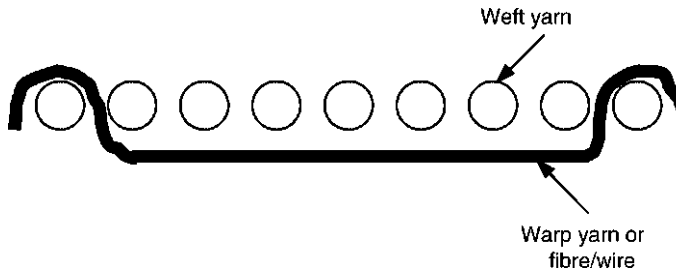

6.15 Schematic of cross-sectional 8-harness satin woven structure.

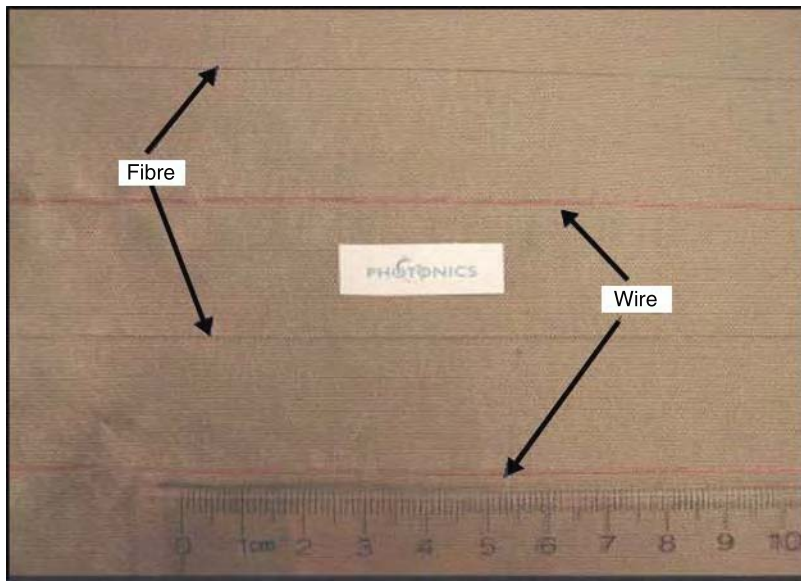

6.16 Different types of optical fibres and electronic wires integrated into a plain-woven structure at 80 PPI.

regular yarn in the warp direction. In the case of integrating fibres/wires into a non-woven fabric, the fibres/wires were sandwiched between layers of fabric, as explained before.

The performance of the integrated fibres and wires was tested to evaluate the process of integration. The optical signals that had been transmitted through integrated fibres were measured and the resistance of the wires was tested. The results show that there was no change in optical signal loss or in wire resistance. Clearly, the integrated optical fibres were not excessively bent or stressed by the fabric yarns. In conclusion, the study thus proved that the methods of integration

that had been developed are suitable for application with the commercially available textile machines. However, minor modifications are recommended for some of the machines (El-Sherif, 2003).

6.5 Applications of smart textiles

Because of the successful integration of optical fibres and fine electric wires into textile structures, a number of applications are under development. One of these applications is the smart parachute, which has the ability to predict the opening forces and to measure the deformation of the fabric of the parachute canopy during airdrops. Smart parachutes with embedded fibre optic sensors can be used for real-time characterisation of the dynamic structural behaviour of parachutes during airdrop (El-Sherif *et al*., 2000a). *In situ* measurements of strain/stress in real time will permit better parachute designs in terms of structural parameters and selection of materials. Another application of smart textiles is the smart uniform, which has the ability to sense environmental conditions. The detection of biological or toxic substances is based on the concept of modifying optical fibres (passive conductors) to become chemically sensitive. This modification is achieved by replacing the passive cladding material in a small section of the optical fibre with a chemically sensitive agent (El-Sherif *et al*., 2000b). When these sensors are incorporated into clothing (such as into uniforms for fire fighters, security guards and special mission personnel), they will provide instantaneous early warning of the presence of chemicals or toxins in the ambient environment (El-Sherif, 2001). A third application of smart textiles is the development of a smart shirt for health monitoring and diagnostics (Park and Jayaraman, 2001). This shirt can be used to monitor heart conditions, blood analysis and circulation, injury conditions, and other health issues. A large number of technical reports and papers have been published, recording the progress achieved thus far on these applications. In the next section, the application of smart textiles in parachutes is discussed.

6.5.1 Smart parachutes

Along with the idea on developing smart structures, an interesting research programme on the development of smart parachutes was carried out by a multidisciplinary team of researchers from the Fibre Optics and Photonics Center of Drexel University and Photonics Laboratories Inc., Philadelphia, Pennsylvania. Two types of fibre optic sensors were developed and applied for sensing static and dynamic loads in parachute canopy and suspension lines (El-Sherif *et al*., 1999, 2001a). One of these types is the optical-fibre Bragg grating (FBG) sensor, which is used as a short-strain gauge for measuring axial strain fibres. The second type of fibre optic sensor that has been developed is based on measurements of modal power distribution (MPD) in multimode fibres. This sensor has the advantages of being inexpensive, highly sensitive, flexible and very small, which are the

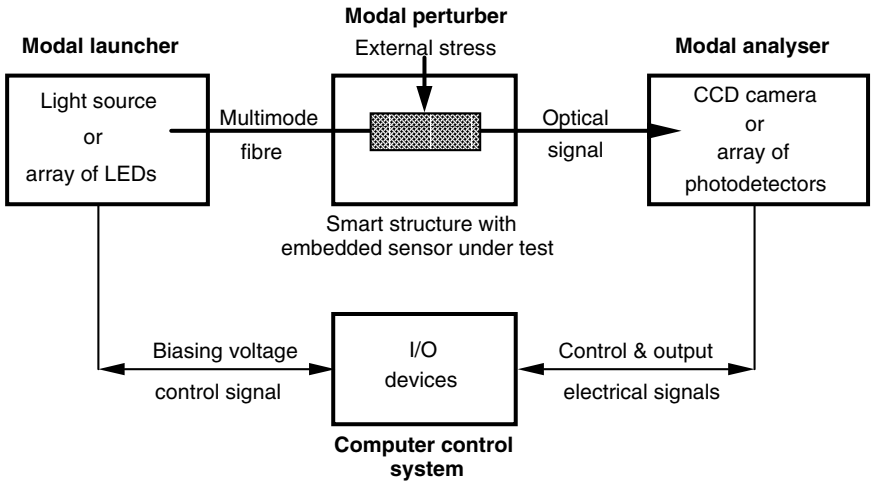

6.17 Function diagram of an application of a MPD sensor system.

requirements for sensors embedded in textile structures (El-Sherif, 1989; El-Sherif *et al*., 1999). It can be used to measure axial as well as transverse strains. When integrated, these two types of sensors form a novel *in situ* monitoring system capable of measuring the dynamic structural behaviour of parachutes during inflation (El-Sherif *et al*., 2001b). Since the application of FBGs as strain sensors is well known and has been reported elsewhere, the principle of operation of the developed MPD sensor will be presented next.

The principle of operation of the MPD technique that has been developed is based on modulating the modal power in multimode fibres. Within a multimode optical fibre, optical signals propagate according to the modal structure of the fibre and the boundary conditions. The MPD within a multimode fibre is a function of the geometry (size) and the optical properties (core and cladding indices) of the fibre and the light-launching conditions. Altering the boundary conditions of an optical fibre induces modal coupling, resulting in the modulation of the modal power distribution (MPD) (Radhakrishnan and El-Sherif, 1996). The Coupled Mode Theory can be employed for the analysis of the MPD modulation (Snyder, 1972; Snyder and Love, 1983).

Deforming the fibre by mechanical stress or other forms of perturbation results in the modulation of modal power, which can be exploited for sensing the applied signals. The measurements of the distribution and subsequent redistribution of the modal power can be accomplished by scanning the far-field pattern at the end of the fibre, using a charged coupled devices (CCD) camera or an array of photodetectors (Fig. 6.17). As an example, for an optical fibre with a core diameter of 20 μm, $n_{clad} = 1.45$ and $n_{core} = 1.46$, the field of the modal power for LP_{lm} modes

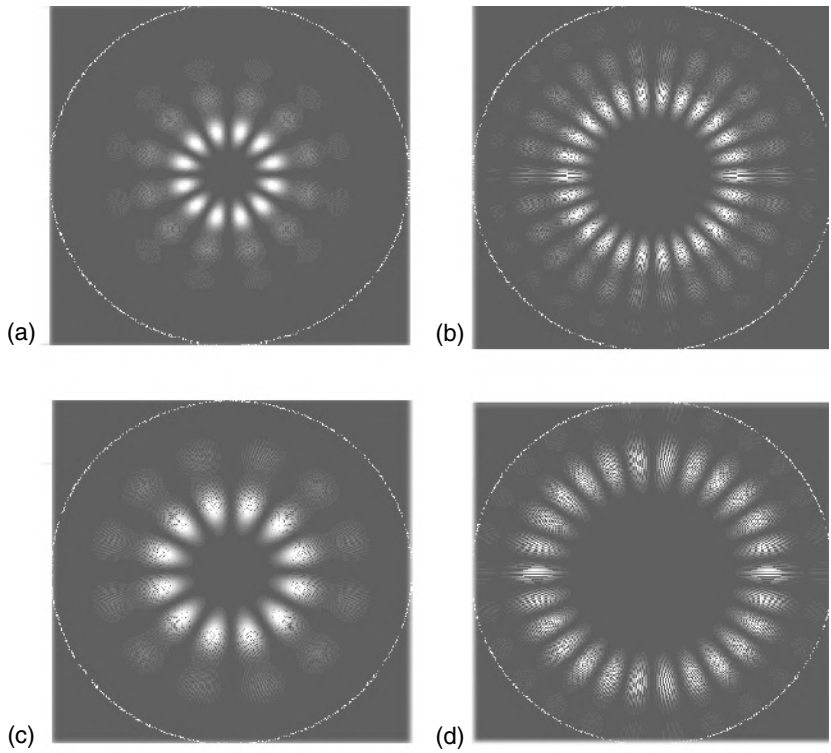

6.18 The LP_{lm} modal structure of a multimode fibre having; n_{core} = 1.46 and (a) l = 6, n_{clad} = 1.45, (b) l = 13, n_{clad} = 1.45, (c) l = 6, n_{clad} = 1.455, and (d) l = 13, n_{clad} = 1.455.

is shown in Fig. 6.18(a) and (b) for the modal orders l = 6 and l = 13, at an optical wavelength of $\lambda = 0.75$ μm. In the presence of external perturbation applied to the fibre resulting in a change of the cladding index to n_{clad} = 1.455, the modal power redistribution of l = 6 and l = 13 modes is shown in Fig. 6.18(c) and (d). This theoretical analysis is based on the use of a single-frequency (laser) light source. However, when a light-emitting diode (LED) is used, the modal power structure will have a continuous distribution of intensity. Through selective excitation, a limited number of propagating modes can be excited. This method can be applied by exciting the optical fibre with a beam of light off-axis.

For example, a step-index silica fibre with a diameter of 100 μm was excited at 10 degrees off-axis, using an LED. The two dimensional far-field pattern (MPD) and intensity profile were scanned and recorded by a CCD camera, as shown in Fig. 6.19(a). When the fibre was under stress, the recorded far-field pattern shows inter modal coupling and a redistribution of the modal power, Fig. 6.19(b). As the applied stress was increased, considerable rearrangement of the modal power was

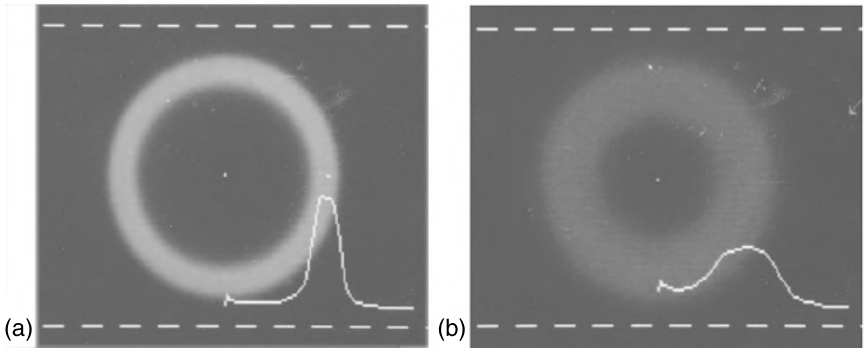

6.19 Far-field pattern and the intensity profile at the end of an optical fibre excited off-axis, (a) before and (b) after a stress was applied to the fibre.

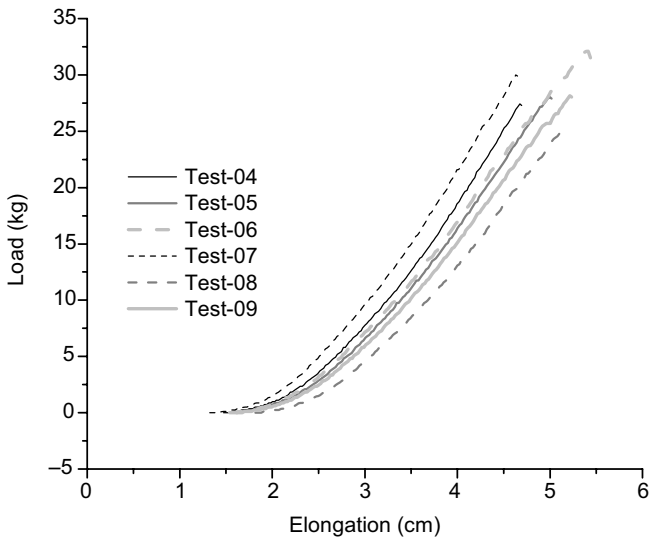

6.20 Tensile tester outputs for the six tested samples, for fabric align along 45 degrees, optical fibre stitched vertically.

recorded. These figures indicate that continuously varying the applied stress will result in continuous changes in the MPD.

For a simple approach and cost-effective sensor configuration, the CCD camera can be replaced by photodetectors located at key positions in the far field. Therefore, using an LED as the light source and regular photodiodes for detection will produce a sensitive, inexpensive and miniature sensor. These advantages make the MPD technique the most suitable one for use in parachute applications.

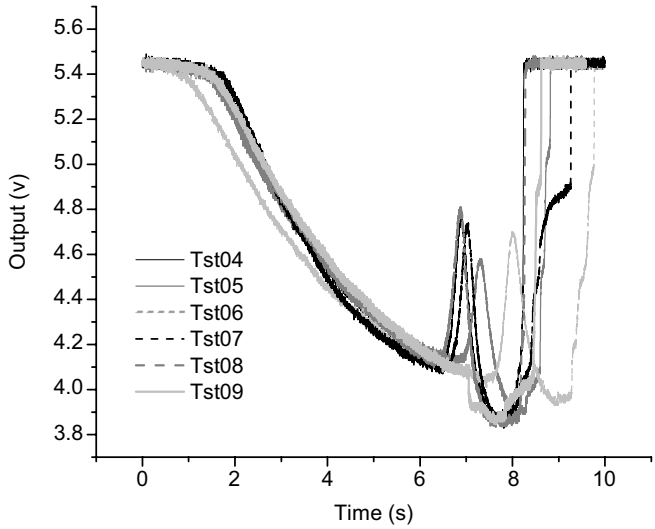

6.21 Optical sensors output for the six tested samples. MPD tensile test for fabric align along 45 degrees, optical fibre stitched vertically.

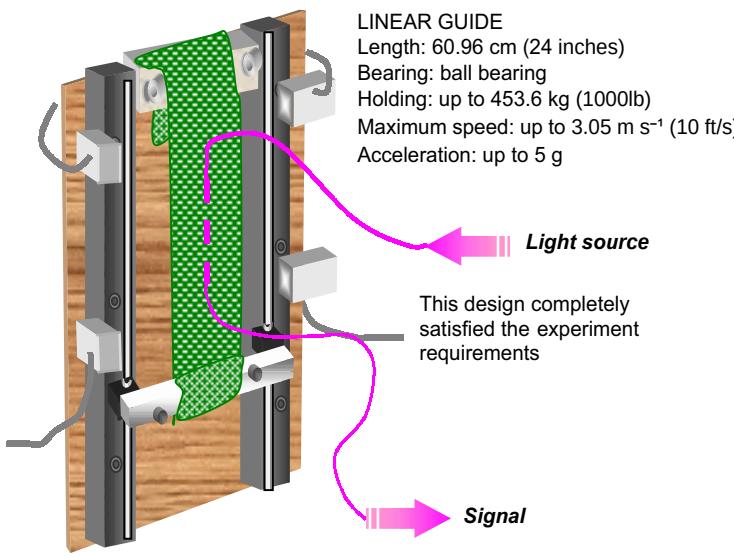

6.22 Experimental setup designed for free-falling drop tests.

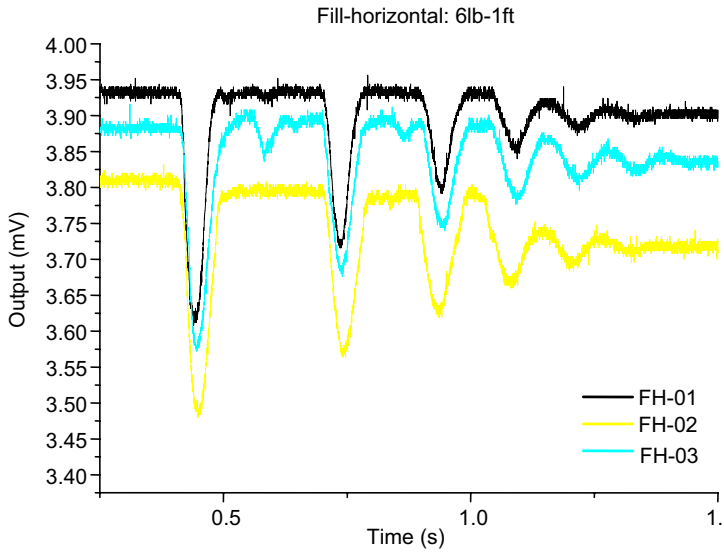

6.23 Drop test results of MPD sensors for three samples.

Experimental work was carried out to validate the MPD technique for measuring static and dynamic strains in textile structures. Quasi-static and dynamic tests were performed on processed samples. Strands of optical fibres were stitched into small pieces of a canopy nylon fabric and tested. The quasi-static test results are used to build the relationship between the optical signal and the mechanical behaviour of the fabric, and thus to predict the external perturbation on the smart fabric during dynamic applications (El-Sherif *et al*., 2001a).

The quasi-static tests were carried out in a uniform, systematic way. The tensile tester pulled the fabric by a certain amount and the output data were then recorded for load, elongation and sensor output. This process was continued until the fabric began to tear. Figure 6.20 shows the tensile tester output (load versus elongation) for six tested samples, and the sensor output is shown in Fig. 6.21. It can be seen that the output of the sensor was in full agreement with the output of the tensile tester for the first 6 s, before the fabrics started to tear.

For dynamic tests, a test setup was designed to study the dynamic behaviour of the parachute fabrics and to develop the instrumentation needed for field applications. A drop test setup was designed, as shown in Fig. 6.22, for free-falling tests. Several tests were carried out using different weights and different dropping distances. In each case, the output of the photodetector was recorded with the use of an oscilloscope. Figure 6.23 shows the output of the photodetector, in terms of voltage versus time, for three samples tested at a weight of 2.72 kg (6 lb) and a drop height of 30.48 cm (1 ft). The sensor output for the three samples is identical. The

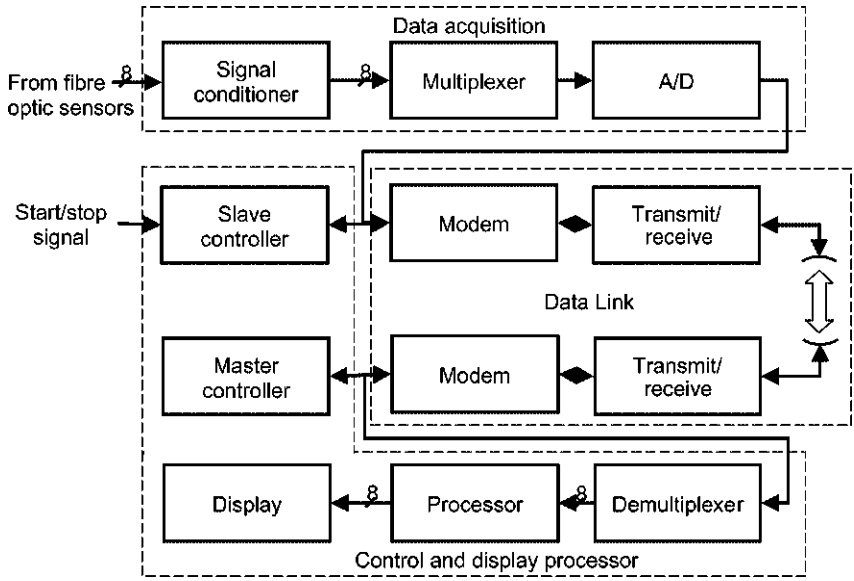

6.24 Schematic diagram of the eight channels RF remote data acquisition system.

first pulse records the output data for the drop test and the following pulses represent information on the oscillation. The tests were repeated for different weight and heights.

The major observation to be deduced from these data is that the height of the first pulse and the number of major pulses increase as the dropping distance increases. A second observation is that the delay time between the first two major pulses increases as the dropping distance increases. This increase in delay time reflects an increase in the time it takes for the load motion to bounce back for the second cycle of oscillation. As a result of these drop tests, a clear relationship exists between the dropping weight and dropping distance on the one hand and the pulse widths, time delay between the first and second pulses, and the number of pulses on the other. The number of experiments conducted was enough to draw the general conclusion on these relationships that the developed methodology can be applied to measure the dynamic strain during the time a parachute inflates. All of the recorded data can be directly translated to determine the amount of strain/stress applied to the fabric of the parachute during drop tests.

Based on the successful results achieved in the laboratory tests (quasi-static and dynamic) and on the mechanical analysis and modelling, a correlation function between the induced strain and the output of the sensors has been developed. Recently, a complete remote sensory system was developed and integrated into a small-scale parachute, and field tests were successfully carried out. The parachute used in the test was one-quarter of the scale of a regular personal circular

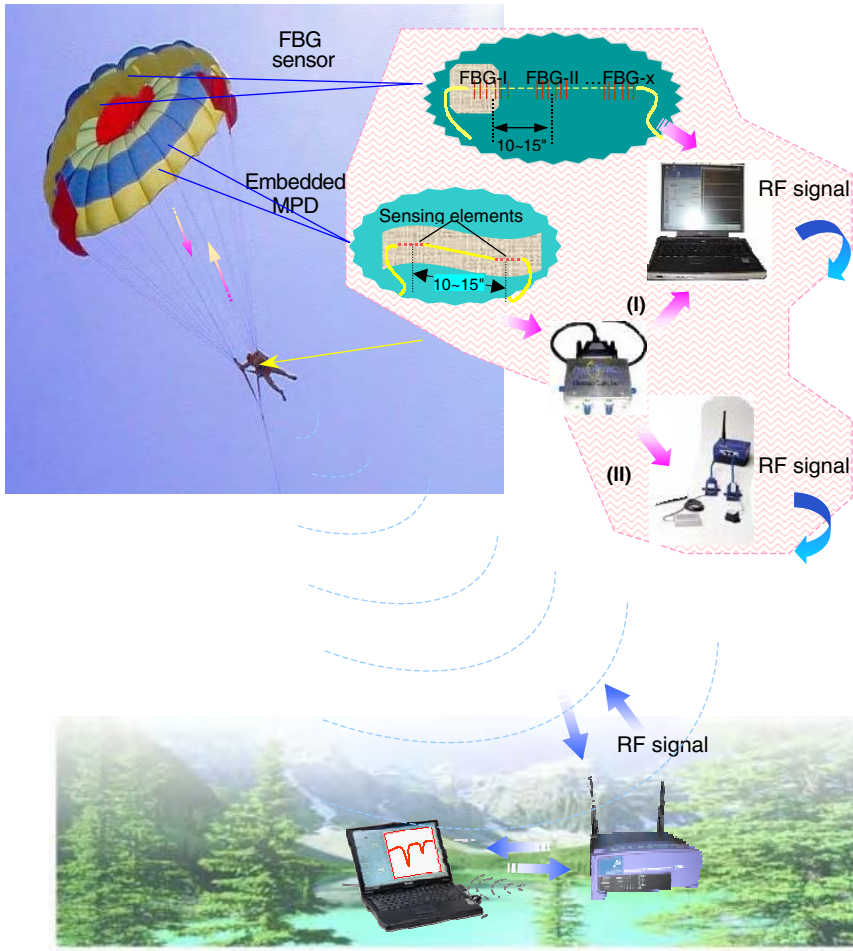

6.25 Schematic diagram of the developed smart parachute, showing the sensor's components, the RF transmitter receiver and the ground station.

parachute. A number of fibre optic sensors were integrated in the canopy of the parachute. Specifically, four sensors of each of the MPD and the FBG types were integrated in the radial and hoop directions of the canopy, two in each direction. For real-time monitoring of the sensor's outputs during the airdrop, an electronic device for data multiplexing was developed in connection with a RF wireless transmitter receiver, to transmit the data to a ground station, as shown in Fig. 6.24. A schematic diagram of the smart parachute with all the equipment and systems that had been developed is shown in Fig. 6.25. Field-drop tests have also recently been successfully carried out. The results have been presented in the Final

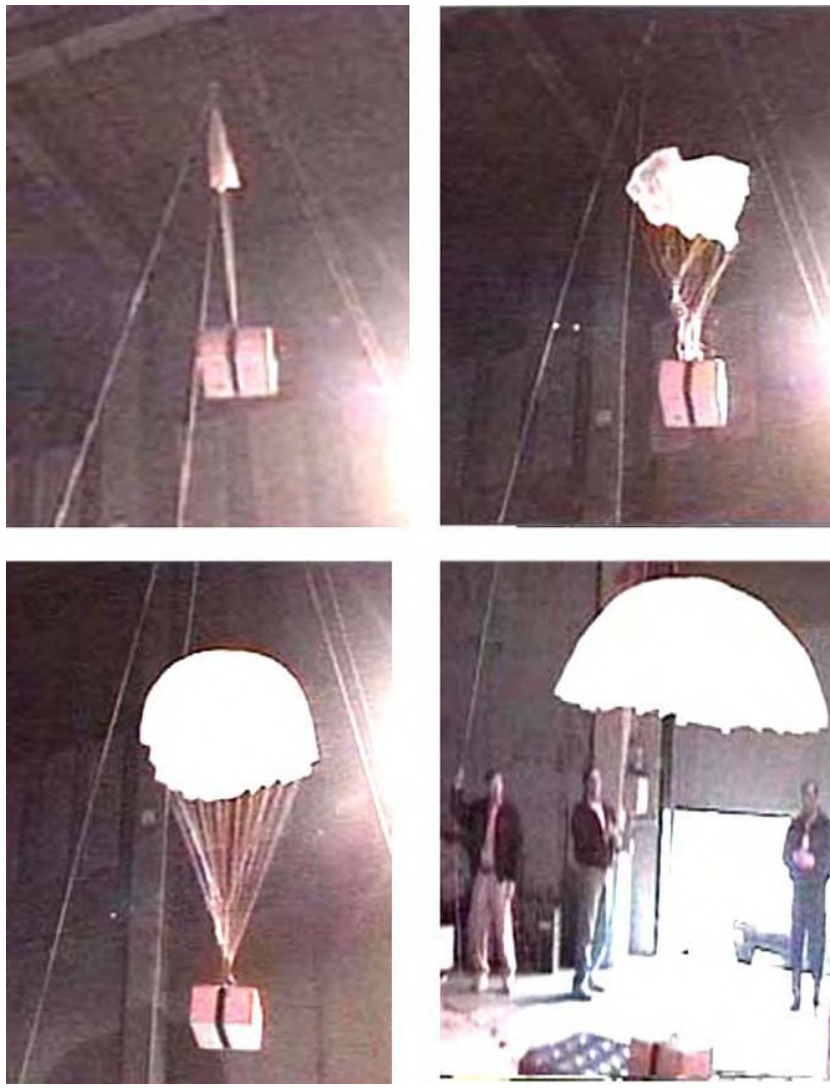

6.26 Scenes of the drop test, showing the parachute load where the sensor's data acquisition electronics and the RF transmitter are located.

Technical Report submitted by Photonics Laboratories, Inc. to the US Army under Contract # DAAD16-01-C-0003 (El-Sherif, 2002b). Various pictures captured during the drop test are shown in Fig. 6.26.

In conclusion, the remote sensory system that has been developed, embedded into the canopy of a parachute, has been proven to operate successfully during field tests. Although the remote sensor system was designed for *in situ* measurement of strain/stress in parachute canopies, it can be used to measure environmental

conditions in spaces if the strain sensors are replaced by fibre optic chemical sensors. The methods developed to manufacture smart parachutes and smart uniforms can be applied to many other textile structures. Also, the methodology that has been developed presents excellent possibilities for the design of wireless fibre optic systems for health monitoring, not only in terms of textile structures but also in other structures and materials. Finally, the value of the MPD technique in textile-embedded sensor applications, where miniature and flexible sensor structures are of great importance, has been successfully demonstrated through these experiments on smart textiles.

6.6 Acknowledgements

Special thanks are accorded to the members of the research team who have worked with me for the past six years at the Fibre Optics and Manufacturing Engineering Center, Drexel University and Photonics Laboratories, Inc., Philadelphia, Pennsylvania, in developing various types of smart textiles. I am most grateful for the technical collaboration and continuous contribution of Jianming Yuan, Min Li, Dina El-Sherif, Mohamed Hidayet, Saif Khalil, Mohamed Abou-iiana, Fuzhang Zhao (for the development of the mechanical analysis), Rachid Gafsi, Kemal Fidanboylu, Lalit Bansal and Bulent Kose. Special appreciation also goes to Calvin Lee and James Fairneny of the US Army Natick Soldier Center, Natick, MA, for their continuous support and technical contribution.

6.7 References

El-Sherif M A (1989) 'On-fiber sensor and modulator,' *IEEE Transactions on Instrumentation and Measurements*, April, 595–598.

El-Sherif M A (1997), 'Fiber Optic Sensors for Soldiers' Smart Uniforms' (invited paper), *Third ARO Workshop on Smart Structures*, Virginia Polytechnic and State University, Blacksburg, Virginia, Aug. 27–29.

El-Sherif M A, Fidanboylu K, El-Sherif D, Gafsi R, Yuan J, Lee C and Fairneny J (1999) 'A novel fiber optic system for measuring the dynamic structural behavior of parachutes', *Fourth ARO (US Army Research Office) Workshop on Smart Structures*, State College, PA, August 16–18.

El-Sherif M A, Fidanboylu K, El-Sherif D, Gafsi R, Yuan J, Lee C and Fairneny J (2000a), 'A novel fiber optic system for measuring the dynamic structural behavior of parachutes', *J. Intell. Mater. Syst. Struct.*, **2**(5), 351–359.

El-Sherif M A, Yuan J and MacDiarmid A G (2000b), 'Fiber optic sensors and smart fabrics,' *J. Intell. Mater. Syst. Struct.*, **2**(5), 407–414.

El-Sherif M, Li M, El-Sherif D and Lee C (2001a), 'Fiber optic system for measuring the structural behavior of parachute airdrop: Quasi-static and dynamic testing, structure health monitoring', Fu-Kuo Chang (ed.), Stanford University, CRC Press, 733–741.

El-Sherif M, El-Sherif D and Lee C K (2001b), *Method and Apparatus for Evaluating Parachutes Under Load*, US Patent 6,299,104 B1.

El-Sherif M A (2001), 'The final technical report on "Sensors and Smart Fabrics",' *The MURI-ARO project on Functionally Tailored Textiles*, Contract #DAAH 04-96-1-0018.

El-Sherif M (2002a), *Manufacturing of Smart Textile Integrating Optical and Electrical Conductors, and Sensors, Phase I*, Technical Report, US Army Contract # DAAD16-01-C-0054.

El-Sherif M (2002b), *A novel fiber optic system for measuring the dynamic structuring behaviour of parachutes, Phase II*, Final technical report, US Army Contract, # DAAD16-01-C-0003.

El-Sherif M (2003), *Manufacturing of smart textile integrating optical and electrical conductors and sensors, Phase II*, Final technical report, US Army Contract, # DAAD16-10-C-0054.

Hearle J W S, Grosberg P and Backer S (1969), *Structural Mechanics of Fibers, Yarns, and Fabrics*, Vol. 1, Wiley-Interscience, New York.

Olofsson B (1964), 'A general model of a fabric as a geometric–mechanical structure', *J. Textile Inst*., **55**(11), T541–T557.

Park S and Jayaraman S (2001), 'Adaptive and responsive textile structures (ARTS)', Tao X M (ed), *Smart Fibers, Fabrics and Clothing: Fundamentals and Applications*, Woodhead Publishing, Cambridge, England.

Peirce F T (1937), 'The geometry of cloth structure', *J. Textile Inst*., **28**(3), T45–T96.

Radhakrishnan J and El-Sherif M A (1996), 'Analysis on spatial intensity modulation for fiber optic sensor applications', *J. Optical Fiber Technol*., **2**(1), 114–126.

Snyder AW (1972), 'Coupled mode theory for optical fibers', *J. Optical Soc. Amer*., **62**(11), 1267–1277.

Snyder A W and Love J D (1983), *Optical Waveguide Theory*, Chapman and Hall, London.

Zhao F, Abou-iiana M and El-Sherif M, 'Smart textiles integrating optical and electrical conductors – a fabric model for plain weaving', in press.

6.8 Bibliography

Buck J A (1995), *Fundamentals of Optical Fibers*, John Wiley & Sons, New York.

Collins G E and Buckley L J (1996), 'Conductive polymer-coated fabrics for chemical sensing', *Synth. Metals*, **78**, 93–101.

Croll R H, Klimas P C, Tate R E and Wolf D F (1981), 'Summary of parachute wind tunnel testing methods at Sandia National Laboratories', *7th AIAA Aerodynamics & Balloon Technical Conference*, San Diego, CA, Oct. 21–23, Paper No. 81–1931.

El-Sherif M A *et al*. (1990), 'Modal power distribution modulation for sensor applications', *Technical Digest of Annual Meeting*, Optical Society of America (OSA), Boston, Nov. 4–9.

El-Sherif M A and Yuan J (1999), 'Fiber optic sensors and smart fabrics', *Fourth ARO (US Army Research Office) Workshop on Smart Structures*, State College, PA, August 16–18.

El-Sherif M, Fidanboylu K, El-Sherif D, Gafsi R and Lee C (2000), 'A novel fiber optic system for measuring the dynamic forces in textiles, optical fiber sensors', *SPIE*, **4185**, 696–699.

El-Sherif M, Li M, Yuan J, El-Sherif D, Rahman A, Khalil S, Bansal L, Abou-iiana M, Lee C and Fairneny J (2002), 'Smart textiles with embedded opto-electronic networks and sensors – an overview', *International Interactive Textiles for the Warrior Conference*, Soldier Biological and Chemical Command, US Army Natick Soldier Center, Boston, Cambridge, MA, July, 9–11.

Garrard W L and Konicke T A (1981), 'Stress measurements in bias-constructed parachute

canopies during inflation and at steady state', *J. Aircraft*, **18**(10), 881–886.
Garrard W, Konicke M L, Wu K S and Muramoto K K (1987), 'Measured and calculated stress in a ribbon parachute canopy', *J. Aircraft*, **24**(2), 65–72.
Jorgersen D S and Cokrell D J (1981), 'Aerodynamics and performance of cruciform parachute canopies', *AIAA 7th Aerodynamics & Balloon Technical Conference*, San Diego, CA, Oct. 21–23, Paper No. 81–1919.
Lee C K (1984), 'Experimental investigation of full-scale and model parachute opening', *AIAA 8th Aerodynamics & Balloon Technical Conference*, Hyannis, MA, pp. 215–223, April 2–4, Paper no. 84–0820.
MacDiarmid A G, Zhang W J, Feng J, Huang F and Hsieh B R (1998), 'Application of thin films of conjugated oligomers and polymers in electronic devices', *Polymer Preprints*, **339**(1), 82.
Rubber M F (1985), 'Polyurethane-diacetylene elastomers: a new class of optically active materials', *ACS Polym. Mater. Sci. Eng. Preprints*, **53**, 683–688.
Rubber M F (1996), 'Novel optical properties of polyurethane-diacetylene segmented copolymer', *ACS Polym. Mater. Sci. Eng.*, **54**, 665–669.
Saleh B E A and Teich M C (1991), *Fundamentals of Photonics*, John Wiley, New York.
Yuan J, Feng J, El-Sherif M and MacDiarmid A G (1998), 'Development of an on-fibre chemical vapor sensor', *OSA Annual Meeting*, Baltimore, MD, Oct. 4–9.